Solid State Communications 149 (2009) 425–428

Contents lists available at ScienceDirect

Solid State Communications

journal homepage: www.elsevier.com/locate/ssc

Ab initio study of the electronic and atomic structure of the wolframite-type $ZnWO_4$

A. Kalinko [a,*], A. Kuzmin [a], R.A. Evarestov [b]

[a] Institute of Solid State Physics, University of Latvia, Kengaraga Street 8, LV-1063 Riga, Latvia

[b] Department of Quantum Chemistry, St.Petersburg State University, 26 Universitetskiy Prospekt, Stary Peterhof 198504, Russia

ARTICLE INFO

Article history:
Received 2 October 2008
Received in revised form
30 December 2008
Accepted 4 January 2009 by
J.R. Chelikowsky
Available online 10 January 2009

PACS:
71.15.Ap
71.20.Ps

Keywords:
A. $ZnWO_4$
C. Ab initio calculations
D. Electronic band structure

ABSTRACT

Ab initio quantum chemistry calculations of the structural and electronic properties of monoclinic wolframite-type $ZnWO_4$ crystal have been performed within the periodic linear combination of atomic orbitals (LCAO) method using six different Hamiltonians, based on density functional theory (DFT) and hybrid Hartree-Fock-DFT theory. The obtained results for optimized structural parameters, band gap and partial density of states are compared with available experimental data, and the best agreement is observed for hybrid Hamiltonians. The calculations show that zinc tungstate is a wide band gap material, with the direct gap about 4.6 eV, whose valence band has largely O 2p character, whereas the bottom of conduction band is dominated by W 5d states.

1. Introduction

Zinc tungstate $ZnWO_4$ is a technologically important material, which can be used in applications such as scintillators, laser hosts, optical fibers, sensors and phase-change optical recording [1–5].

The crystal structure of $ZnWO_4$ has been determined by neutron [6] and X-ray powder diffraction [7]. $ZnWO_4$ has the monoclinic wolframite-type structure with the space group $P2/c$. There are two formula units per primitive cell, having the lattice parameters $a = 4.69263$ Å, $b = 5.72129$ Å, $c = 4.92805$ Å and $\beta = 90.6321°$ [6]. The presence of two non-equivalent oxygen atoms is responsible for three pairs of Zn–O and W–O bonds, having different lengths. Thus, both Zn and W atoms are surrounded by six oxygens, forming distorted octahedral coordination. The WO_6 octahedra distortion has been directly observed by the W L_3-edge X-ray absorption spectroscopy in [8].

The lattice dynamics of $ZnWO_4$ has been probed by Raman scattering in [9,10] and interpreted on the basis of the octahedral WO_6 groups vibrations. The luminescent properties of $ZnWO_4$ have been widely studied [11–14] and are determined by a charge-transfer between oxygen and tungsten ions in the WO_6 molecular complex [15].

The electronic structure of $ZnWO_4$ has been scarcely studied. A cluster discrete variational $X\alpha$ (DV-$X\alpha$) method has been used in [16] to understand the origin of the valence and conduction bands. It has underestimated the value of the band gap (2.63 eV calculated versus 4.6 eV [11] and 4.9 eV [16] experimental), but was rather successful in describing X-ray photoelectron spectrum (XPS) [16].

Recently, the electronic structure of $[WO_6]^{6-}$–Zn^{2+} complex in $ZnWO_4$ crystal has been calculated by the configuration interaction method in embedded cluster approach to explain the intrinsic luminescence of tungstate [17]. The influence of point defects as oxygen and zinc vacancies on the electronic structure of the complex has been also studied [17].

To the best of our knowledge, the band structure calculations of wolframite-type $ZnWO_4$ have been not performed until now.

In the present work, we have calculated structural and electronic parameters of wolframite-type $ZnWO_4$ crystal, using the periodic linear combination of atomic orbitals (LCAO) method. The obtained results are compared with low-temperature X-ray diffraction data [7] and X-ray photoelectron spectrum [16].

* Corresponding author.
E-mail address: akalin@latnet.lv (A. Kalinko).
URL: http://www.cfi.lv/ (A. Kalinko).

0038-1098/$ – see front matter © 2009 Elsevier Ltd. All rights reserved.
doi:10.1016/j.ssc.2009.01.003

Fig. 1. Band structure diagram (left panel) and total/projected density of states (right panel) for wolframite-type $ZnWO_4$. The energy zero is set at the Fermi energy level.

2. Computational details

The electronic structure and properties of $ZnWO_4$ crystal were carried out using the CRYSTAL06 code [18]. In this approach, the linear combination of localized Gaussian-type atomic orbitals is used to construct Bloch sums as basis functions for the crystalline orbitals. To avoid core electrons of tungsten and zinc atoms, the effective core potentials (ECP) from [19,20] have been chosen: the large core ECP68 for W ($Z = 74$) atom (68 electrons in the core) and the small core ECP18 for Zn ($Z = 30$) atom (18 electrons in the core). Note that the Hay-Wadt ECP68 [19] has been used to describe the structural and electronic properties of bulk tungsten trioxide WO_3 and to explain the observed instability of cubic WO_3 [21], providing the good agreement between the calculated structural parameters for tetragonal WO_3 and available experimental data. The use of ECP18 allows us to include Zn 3d-electrons in the valence shell, which is known to be important for the transition metal compounds. The basis set [20], corresponding to ECP18 pseudopotential, was chosen for Zn atom, and the diffuse Gaussian type orbitals with exponents less than 0.06 were excluded to avoid the basis set linear dependence. The basis set, optimized in the calculations of the cubic WO_3 crystal [21], was adopted for W atom. The all electron basis set, optimized in earlier calculations of perovskites [22], was used for O atoms.

In the CRYSTAL06 code, the accuracy in the evaluation of the Coulomb and exchange series is controlled by a set of tolerances, which were taken to be the default values (6, 6, 6, 6, 12). The Monkhorst-Pack scheme [23] for $8 \times 8 \times 8$ k-point mesh in the Brillouin zone was applied. The total spin projection $S_z = 0$ was fixed in the calculation of the closed shell ground state of insulating $ZnWO_4$ crystal. The SCF calculations were performed for three pure DFT (LDA [24], PW91 [25], PBE [26]) Hamiltonians and three hybrid HF-DFT (B3PW [27], B3LYP [28], PBE0 [29]) Hamiltonians.

3. Atomic structure

In this section, we present the results of the lattice parameters and atomic fractional coordinates optimization for different Hamiltonians in comparison with available experimental data. The optimized values of structural parameters are given in Table 1. The experimental data were obtained from low-temperature (12 K) X-ray diffraction [7].

A sum of squared differences between calculated and experimental structural parameters was used to compare results for different Hamiltonians. All parameters were divided into three groups: the first group consists of three lattice constants (a, b, c), the second one contains the angle β, and the third one contains three atomic fractional coordinates (x, y, z). Lattice constants and atomic fractional coordinates are best reproduced by LDA and PBE0 Hamiltonians, whereas the value of the angle β agrees best of all in the case of hybrid HF-DFT B3PW and PBE0 Hamiltonians. The differences for the three lattice constants do not exceed 4%, the angle β is reproduced within 2%, and atomic fractional coordinates within 14%. Taking into account the differences for all parameters, the hybrid HF-DFT PBE0 Hamiltonian produces the best overall agreement with experimental data [7], and therefore we will further discuss only results based on it.

4. Electronic structure and chemical bonding

In this section, the electronic band structure, projected density of states (PDOS) and difference electron density maps are discussed.

The calculated energy dispersion curves and PDOS for hybrid HF-DFT PBE0 Hamiltonian are shown in Fig. 1. The dispersion curves are plotted along eight different symmetry directions in the Brillouin-zone. Note that the band structure diagrams for other Hamiltonians have qualitatively similar appearance, but have significant difference in the band gap value (Table 1), which is significantly smaller in pure DFT Hamiltonians, as expected [30].

The narrow subband, observed at about −9 eV, corresponds to the Zn 3d states and is well separated from other bands. The upper part of the valence subband (−7.5–0 eV) is due to mostly O 2p states, mixed with W 5d states, whereas the lower part is composed of the O 2p, W 5d with some admixture of Zn 4s states. The highest state in the valence band for pure DFT methods is located at the B point, while the states at Γ, Y and A points are very close in the energy values. A similar situation occurs for hybrid Hamiltonians. However, here the highest state is located at Y point. The bottom of the conduction band is composed mostly of W 5d states. However, an admixture of O 2p and some of Zn 4s states is clearly observed along the conduction band. The lowest energy state in the conduction band is located at Y point of the Brillouin-zone for all Hamiltonians.

Table 1
Comparison of lattice parameters (a, b, c, β) and atomic fractional coordinates (x, y, z), calculated using LDA, PW91, PBE, B3PW, B3LYP and PBE0 Hamiltonians, with the low-temperature (12 K) X-ray diffraction data from [7] for wolframite-type $ZnWO_4$. The total atomic charges (Q), following a Mulliken population analysis scheme, are also given. The experimental values of the energy band gap E_g was taken from [11,16].

	LDA	PW91	PBE	B3PW	B3LYP	PBE0	Exp
a (Å)	4.606	4.696	4.705	4.669	4.693	4.660	4.683
b (Å)	5.702	5.909	5.928	5.840	5.947	5.805	5.709
c (Å)	4.795	4.866	4.870	4.831	4.857	4.820	4.923
β (°)	88.74	88.95	89.05	89.45	89.32	89.62	90.54
Zn (y)	0.687	0.695	0.698	0.697	0.700	0.697	0.681
W (y)	0.205	0.207	0.206	0.202	0.205	0.201	0.181
O1 (x)	0.221	0.220	0.220	0.218	0.219	0.218	0.230
O1 (y)	0.896	0.895	0.895	0.895	0.893	0.895	0.885
O1 (z)	0.449	0.458	0.458	0.454	0.459	0.453	0.430
O2 (x)	0.253	0.247	0.247	0.246	0.245	0.247	0.269
O2 (y)	0.387	0.382	0.382	0.379	0.378	0.379	0.380
O2 (z)	0.409	0.409	0.410	0.408	0.409	0.407	0.406
Q (Zn)	1.48	1.50	1.50	1.55	1.54	1.57	–
Q (W)	3.58	3.52	3.51	3.72	3.76	3.75	–
Q (O1)	−1.32	−1.30	−1.30	−1.37	−1.38	−1.38	–
Q (O2)	−1.22	−1.21	−1.21	−1.27	1.28	−1.28	–
E_g (eV)	2.31	2.33	2.31	4.27	4.22	4.60	4.6, 4.9

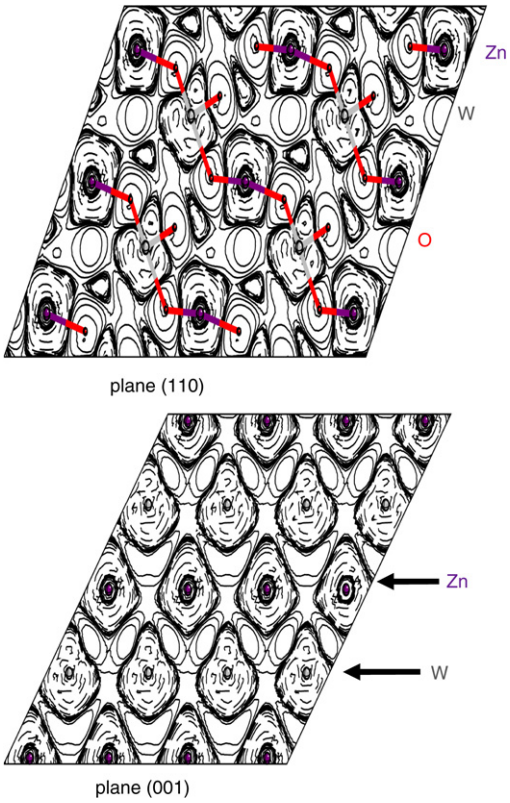

Fig. 2. (Color online) Difference electron density maps in (001) (top plot) and (110) (bottom plot) planes for wolframite-type $ZnWO_4$. Solid, dashed, and dot-dashed lines correspond to positive, negative and zero difference, respectively.

To conclude, the minimum band gap for PBE0 Hamiltonian, which is the best in the reproduction of structural parameters, occurs at Y point of the Brillouin-zone and corresponds to a direct transition. The calculated band gap value $E_g = 4.6$ eV is in good agreement with the experimental values 4.6 eV [11] and 4.9 eV [16].

In Fig. 2, we show the difference electron density maps in the two most representative (001) and (110) planes. The (001) plane passes through Zn, W and three O atoms. One can see that the electron density around W atom is distorted due to a displacement of the W atoms from the center of oxygen octahedra, caused by the second order Jahn–Teller effect. The electron density around Zn atoms is relatively symmetric. The second (110) plane passes through Zn and W atoms only. There is electron density distortion around both atoms, indicating that oxygen octahedra around Zn atoms are also deformed.

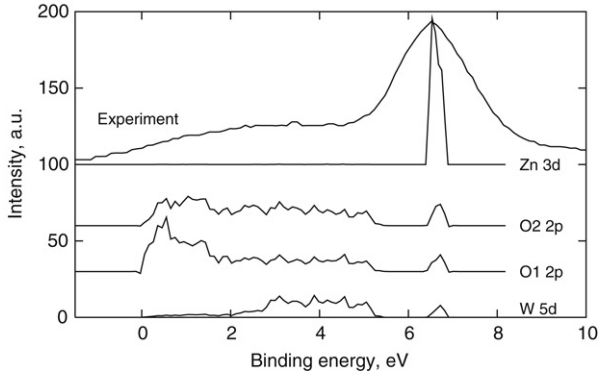

Fig. 3. Comparison of XPS spectrum and PDOS curves for wolframite-type $ZnWO_4$. Curves are vertically shifted for clarity.

The comparison between XPS spectra [16] and PDOS curves calculated using PBE0 is shown in Fig. 3. The binding energy of PDOS curves is given relative to the Fermi level placed at the top of the calculated valence band. The energy scale of the XPS spectrum has been modified for the best agreement of the main sharp peak in the experimental signal with the Zn 3d PDOS position. The low binding energy broad peak of the XPS spectrum is attributed to the O 2p states, with some admixture of the W 5d states. The overall agreement between calculated splitting of the O 2p states and Zn 3d states and the two peaks in the XPS spectrum is very good, being better than that found previously within the cluster DV-$X\alpha$ method [16].

5. Conclusions

Ab initio calculations of the structural and electronic properties of wolframite-type $ZnWO_4$ crystal have been performed within the periodic LCAO method using six different Hamiltonians, based on density functional theory (DFT) and hybrid Hartree-Fock-DFT theory. The results obtained for all Hamiltonians differ from experimental values less than 14%, while all structural and electronic parameters are best reproduced by hybrid PBE0 Hamiltonian. Tungsten–oxygen chemical bonding is covalent due to the electron density transfer to oxygen atoms, whereas zinc atoms show more ionic behavior. Calculated density of states is in

good agreement with XPS spectrum. The main contribution to the valence band is due to the Zn 3d states at high binding energies and the O 2p and W 5d characters at low and medium binding energies.

Acknowledgment

This work was partially supported by Latvian Government Research Grant No. 05.1717.

References

[1] H. Wang, F.D. Medina, D.D. Liu, Y.D. Zhou, J. Phys: Condens. Matter 6 (1994) 5373.
[2] H. Kraus, V.B. Mikhailik, Y. Ramachers, D. Day, K.B. Hutton, J. Telfer, Phys. Lett. B 610 (2005) 37.
[3] H. Grassmann, H.G. Moser, E. Lorenz, J. Lumin. 33 (1985) 21.
[4] A.R. Phani, M. Passacantando, L. Lozzi, S. Santucci, J. Mater. Sci. 35 (2000) 4879.
[5] A. Kuzmin, R. Kalendarev, A. Kursitis, J. Purans, J. Non-Cryst. Solids 353 (2007) 1840.
[6] P.F. Schofield, K.S. Knight, G. Cressey, J. Mater. Sci. 31 (1996) 2873.
[7] H. Kraus, V.B. Mikhailik, L. Vasylechko, D. Day, K.B. Hutton, J. Telfer, Yu. Prots, Phys. Status Solidi (a) 204 (2007) 730.
[8] A. Kuzmin, J. Purans, Rad. Measurements 33 (2001) 583.
[9] Y. Liu, H. Wang, G. Chen, Y.D. Zhou, B.Y. Gu, B.Q. Hu, J. Appl. Phys. 64 (1998) 4651.
[10] H. Wang, F.D. Medina, Y.D. Zhou, N.Q. Zhang, Phys. Rev. B 45 (1992) 10356.
[11] V.N. Kolobanov, I.A. Kamenskikh, V.V. Mikhailin, I.N. Shpinkov, D.A. Spassky, B.I. Zadneprovsky, L.I. Potkin, G. Zimmerer, Nucl. Instrum. Methods Phys. Res. A 486 (2002) 496.
[12] L. Grigorjeva, D. Millers, S. Chernov, V. Pankratov, A. Watterich, Rad. Measurements 33 (2001) 645.
[13] V.B. Mikhailik, H. Kraus, G. Miller, M.S. Mykhaylyk, D. Wahl, J. Appl. Phys. 97 (2005) 083523.
[14] S.B. Mikhrin, A.N. Mishin, A.S. Potapov, P.A. Rodnyi, A.S. Voloshinovskii, Nucl. Instrum. Methods Phys. Res. A 486 (2002) 295.
[15] V. Nagirnyi, E. Feldbach, L. Jönsson, M. Kirm, A. Kotlov, A. Lushchik, V.A. Nefedov, B.I. Zadneprovski, Nucl. Instrum. Methods Phys. Res. A 486 (2002) 395.
[16] M. Itoh, N. Fujita, Y. Inabe, J. Phys. Soc. Jap. 75 (2006) 084705.
[17] Yu.A. Hizhnyi, T.N. Nikolaenko, S.G. Nedilko, Phys. Status Solidi (c) 4 (2007) 1217.
[18] R. Dovesi, et al. Crystal06, Users manual, University of Turin, 2006.
[19] P.J. Hay, W.R. Wadt, J. Chem. Phys. 82 (1985) 270, 284, 299.
[20] M.M. Hurley, L.F. Pacios, P.A. Christiansen, R.B. Ross, W.C. Ermler, J. Chem. Phys. 84 (1986) 6840.
[21] F. Cora, A. Patel, N.M. Harrison, R. Dovesi, C.R. Catlow, J. Amer. Chem. Soc. 118 (1996) 12174.
[22] S. Piskunov, E. Heifets, R.I. Eglitis, G. Borstel, Comput. Mater. Sci. 29 (2004) 165.
[23] H.J. Monkhorst, J.D. Pack, Phys. Rev. B 13 (1976) 5188.
[24] S.H. Vosko, L. Wilk, M. Nusair,Can, J. Phys. 58 (1980) 1200.
[25] J.P. Perdew, J.A. Chevary, S.H. Vosko, K.A. Jackson, M.R. Pederson, D.J. Singh, C. Fiolhais, Phys. Rev. B 46 (1992) 6671.
[26] J.P. Perdew, K. Burke, M. Ernzerhof, Phys. Rev. Lett. 77 (1996) 3865.
[27] J.P. Perdew, Electronic Structure of Solids, Akademie Verlag, Berlin, 1991.
[28] A.D. Becke, J. Chem. Phys. 98 (1993) 5648.
[29] C. Adamo, V. Barone, J. Chem. Phys. 110 (1999) 6158.
[30] R.A. Evarestov, Quantum Chemistry of Solids, Springer, Berlin, 2007.